Magnetic properties of poly(*p*-xylylene)-Ni nanocomposites

Artem Vdovichenko[1,2,⋆], *Dmitry* Streltsov[1,2], *Anton* Orekhov[1], *Alexander* Vasiliev[1], *Yan* Zubavichus[1], *Evgenii* Grigoriev[1], *Sergei* Zavyalov[1], *Leonid* Oveshnikov[1,3], and *Sergei* Chvalun[1,2]

[1] *National Research Center "Kurchatov Institute", 123182 Moscow, Russia*
[2] *N.S. Enikolopov Institute of Synthetic Polymer Materials RAS, 117393 Moscow, Russia*
[3] *P.N. Lebedev Physical Institute RAS, 119991 Moscow, Russia*

Abstract. The dependence of electrical and magnetic properties on structure of thin poly(*p*-xylylene) - nickel nanocomposite films with Ni concentrations from 5 to 30 vol.% was studied. It was found that metal concentration strongly affects size and oxidation state of the nanoparticles. Effect of the filler content on electrical and magnetic properties of the nanocomposites was revealed. These properties are determined by percolation phenomenon, with the percolation threshold value of about 10 vol.%. The well pronounced magnetic hysteresis as well as ferromagnetic ordering were observed at Ni content above the percolation threshold. The diagrams of magnetic properties of these composites as a function of composition and temperature were elaborated.

1 Introduction

Magnetic polymer nanocomposites are perspective materials due to possibility to combine several components with different properties in a single material. Organic-inorganic synergies add new properties that cannot be achieved in just organic or inorganic materials. Furthermore, when magnetic particles are of nano-size its magnetic properties are different qualitatively from the bulk material, they vary with the particle size, and can be affected by the polymer interphase. A lot of papers on magnetic, magnetoresistive properties of the polymer nanocomposites and spintronic devices have been published revealing recent progress in spintronics research [1–6].

Spin-valve structures are the subject of special interest in these studies [7]. The devices employing the effect of the giant (or tunneling) magnetoresistance are generally three layer systems. A non-magnetic layer is sandwiched between hard- and soft-ferromagnetic ones. On the basis of such structures magnetoresistive memory cells as well as scanning magnetic heads for high-density HDDs can be produced. It should be noted that polymer materials are often used as the non-magnetic interlayer only [4, 5, 8]. However, the use of single nanocomposite material with embedded magnetic particles in spin-valve applications seems to be technologically promising.

2 Experimental

The poly(*p*-xylylene) (PPX) - Ni nanocomposite films have been prepared by low-temperature vapor deposition polymerization (VDP) technique [9], which is a powerful vacuum deposition technique enabling preparation of thin hybrid nanocomposite films with a high content of inorganic filler (up to several tens of volume percents) [9, 10]. The process is carried out without solvent or catalyst and allows to form nanocomposite films of controllable thickness in the range from several nanometers to several hundred micrometers with sizes of inorganic nanoparticles down to 2 nm and adjustable concentration of the filler.

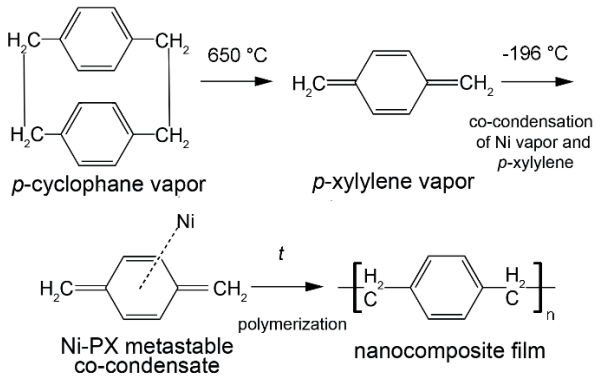

Figure 1. Scheme of synthesis of Ni-PPX nanocomposite films.

The process consists of two stages (see Fig. 1). The first stage is a co-condensation of Ni vapor and *p*-xylylene (PX) monomer on the substrate cooled down to -196 °C. During the deposition, a vacuum better than 10^{-5} Torr was maintained in the VDP chamber. Upon the second stage of the process, during slow heating of the co-condensate up to room temperature, the polymerization of PX into PPX and aggregation of the nickel clusters and atoms into nanoparticles occur. The PX monomer was prepared by pyrolysis of cyclic dimer of PX ([2.2]*p*-cyclophane) (Daisan Kasei, Japan) at 650 °C using classical Gorham's method [11].

⋆e-mail: vdartem@ya.ru

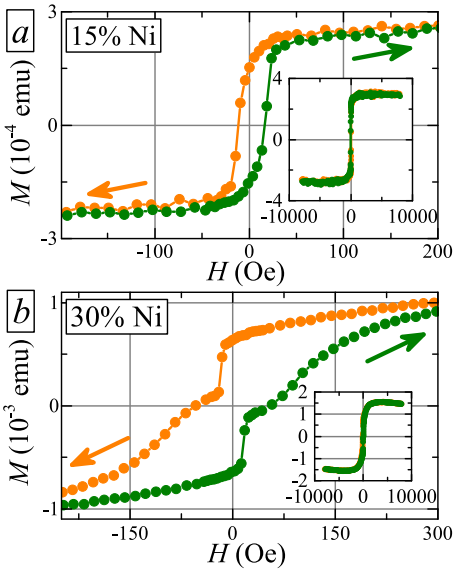

Figure 2. (color online) Magnetic field dependences of magnetic moments for the samples a) 15 vol.% of Ni and b) 30 vol.% of Ni at room temperature (300K). Insets show the same dependences in the wider range of magnetic fields up to 10000 Oe. These curves clearly demonstrate the saturation of magnetization in fields of approximately 200 Oe for the sample 15 vol.% and 4000 Oe for the sample 30 vol.%.

Ni vapor was produced by thermal evaporation. The PPX-Ni samples with Ni concentration in the range from 5 to 30 vol.% were formed. The film thickness was about 300 nm for X-ray diffraction, magnetic and electrical measurements, while for transmission electron microscopy (TEM) studies it was less than 100 nm.

Magnetic properties measurements of the synthesized nanocomposites were carried out with a magnetometer LakeShore 7407 in magnetic fields up to 16000 Oe and with a SQUID magnetometer (Quantum Design, USA) in magnetic fields up to 70000 Oe at temperatures in the range from 4.2 to 300 K. The magnetic field was parallel to the film surface.

The microstuctural analysis was performed in a transmission/scanning electron microscope Titan 80-300 TEM/STEM (FEI, USA). The crystalline structure of the metal/polymer nanocomposites was studied using Rigaku SmartLab (Japan).

3 Results

3.1 Magnetic properties

The synthesized nanocomposite films reveal metal type of conductivity for both 15 and 30 vol.% samples with longitudinal resistance R_{xx} increasing linearly with temperature. The resistivity of the 30 vol.% sample is about $2 \cdot 10^{-3}$ Ohm·cm and the temperature coefficient of resistance $\alpha = 0.015$ K^{-1} is just twice as large as α for bulk nickel.

Fig. 2 presents the dependence of magnetic moment on external magnetic field for two samples with Ni content above the percolation threshold (15 vol.% and 30 vol.%, correspondingly) measured at room temperature. Both samples demonstrate the ferromagnetic behavior showing

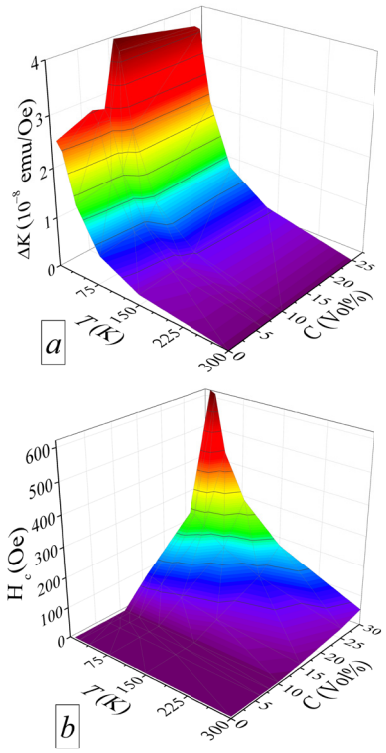

Figure 3. (color online) Temperature and composition dependences of a) ΔK and b) coercive force H_c.

well pronounced magnetic hysteresis. These plots reveal the establishment of long-range ordering and magnetic percolation even in the sample with 15 vol.% of Ni. These observations confirm that the magnetic percolation threshold is less than 15 vol.%.

The magnetization saturates at room temperature at fields of approximately 200 and 4000 Oe for the samples with 15 and 30 vol.% of Ni respectively. The value of the coercive force at room temperature is found to be 13 Oe for the sample with 15 vol.% of Ni and 50 Oe for the sample with 30 vol.% of Ni. The saturation magnetic moment of the sample with 30 vol.% of Ni is more than 5 times higher than that of the sample with 15 vol.% of Ni (see Fig. 2). The difference in magnetic properties of these samples is in agreement with the difference in Ni content taking into account the percolation character of exchange interaction in these type of systems. In particular, such behavior is related to the nonlinear increase of percolation cluster volume at such C values.

The magnetic hysteresis curve of the sample with 30 vol.% of Ni shows narrowing in the vicinity of zero magnetic field, unlike that of the sample with 15 vol.% of Ni (Fig. 2). Such narrowing is typical for ferromagnetic material with wide particle size distribution or at least two fractions of particles of different size because of their different contribution to the sample magnetization. One can explain this observation by wider particle size distribution in the PPX-Ni nanocomposite films with nickel concentration significantly above the percolation threshold, where some metal particles aggregates into bigger clusters while others stay individual. However, if the metal concentration is close to the percolation threshold, fraction of aggregated particles is low compared to individual ones.

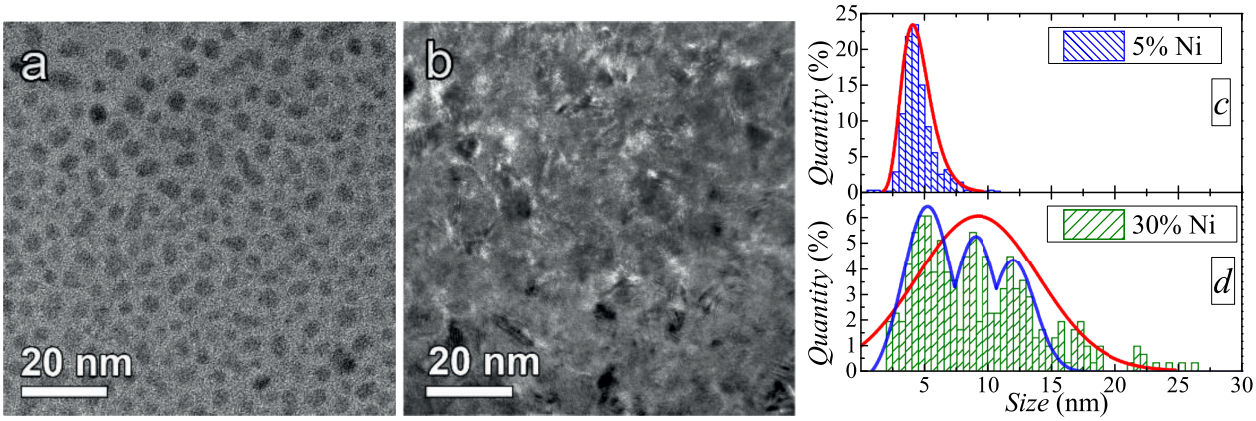

Figure 4. (color online) Bright-field TEM images of the nanocomposite films a) with C = 5 vol.% of Ni and b) 30 vol.% of Ni. c) and d) - corresponding nanoparticle size distributions. Solid curves - normal distribution functions; red - single-modal, blue - multi-modal (see text).

Fig. 3 shows the summarized results of magnetic measurements for the PPX-Ni composite films with various concentrations of nickel. All studied samples including pure PPX film demonstrate linear $M(H)$ dependence for H > 40000 Oe in the temperature range from 150 K down to 10 K. The diamagnetic contribution of substrate was subtracted. Plotting the change of linear slope ΔK as a function of temperature and concentration and using data for pure PPX sample as a reference one can evaluate paramagnetic contribution related to the Ni filler. One can see that an increase of Ni concentration leads to enhancement of paramagnetic response (Fig. 3a). Its magnitude has nonlinear dependence on the filler concentration C, which can be attributed to the presence of oxidized Ni particles (e.g. NiO particles).

$M(H)$ dependences for samples with C > 15 vol.% at low magnetic fields reveal well-pronounced hysteresis loops (see Fig. 2), that have clear temperature dependences. Using the coercive force H_c as a marker of ferromagnetic properties, one can plot corresponding temperature-composition diagram (Fig. 3b). A growth of the nickel concentration C from 15 to 30 vol.% results in an increase of the coercive force H_c at temperatures below 40 K by a factor of 6. Thus, introduction of Ni into PPX matrix leads to an increase of paramagnetic contribution and at C > 15 vol.% ferromagnetic phase is formed, even at room temperature.

3.2 Structure

The magnetic and electrical properties of the PPX-Ni nanocomposite films described above should be caused by structural changes with the increase of Ni content.

The structure of the PPX-Ni nanocomposite films was studied by transmission electronic microscopy (TEM), high resolution TEM (HRTEM), and X-ray diffraction patterns (XRD).

Bright-field (BF) TEM images of the PPX-Ni films with 5 and 30 vol.% of Ni are shown in Fig. 4a and 4b, respectively. In the micrographs, the Ni particles can be identified by a darker appearance. As one can see in Fig. 4a, in the sample with low nickel concentration the metal particles are isolated and homogeneously distributed in the polymer matrix. The nanoparticles are spherical or slightly elongated with the aspect ratio of up to 2. Their average size is about 4-5 nm (see Fig. 4c). The surface density (the number of particles per unit area) is about $3{\cdot}10^{11}\mathrm{cm}^{-2}$. At high filler concentration the inorganic particles are distributed quite uniformly (see Fig. 4b). Their average size is about 8-10 nm, if we assume that their size distribution is also single-modal (see Fig. 4d - red line). Thus, the nanoparticles in studied films with high filler concentration are about twice as big as the ones in the sample with low filler content. However, their density is more or less the same for the samples with 5 and 30 vol.% of Ni. It should be noted that particle size distribution for the sample with 30 vol.% of Ni can be also interpreted as a multimodal while for sample with 5 vol.% of Ni it is clearly single-modal. As an example we provide three-peak line as a guide for an eye, which is just a superposition of three normal distribution curves (see Fig. 4d). One can see that multi-modal curve gives a better fit for present data than single-modal one. The actual number of peaks in multimodal distribution cannot be retrieved from our data, but even a single-modal distribution (being wide enough, as it is in present case) can explain the complex form of hysteresis loop for this sample (see Fig. 2b).

Chemical nature of nanoparticles is of key importance for rationalization of their electrical and magnetic properties. The difference in structure of the PPX-Ni nanocomposites with 5 and 30 vol.% of nickel is mainly related to size of the metal nanoparticles. A two-fold increase in size of the nanoparticles results in a decrease in average distance between adjacent nanoparticles and as a consequence leads to dramatic difference in their electric and magnetic properties.

The X-ray diffraction (XRD) patterns of the samples with 5, 9, and 30 vol.% of Ni are shown in the Fig. 5. The patterns corresponds to those of bulk Ni and NiO crystals. Observed peaks are considerably broadened compared to the single crystal case, which signifies the finite size of nanoparticles.

One can see that sample with Ni concentration of 30 vol.% have peaks at d = 0.203 and 0.178 nm. These peaks are attributed to the planes (111) and (200) respectively of the fcc-lattice of metallic nickel.

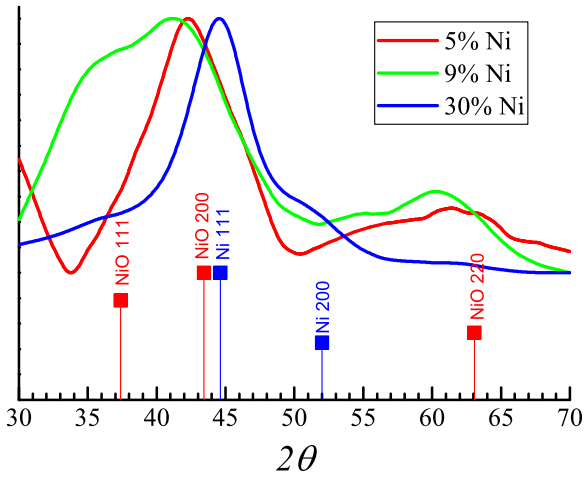

Figure 5. (color online) XRD patterns of three samples with 5 (red), 9 (green), and 30 (blue) vol. % Ni. λ = 1.5406Å.

At concentration 9 and 5 vol.% of Ni the NiO-related peaks in obtained patterns are observed. We can identify these broadened peaks as (111), (200) and (220) planes of NiO.

Therefore, in addition to structural changes observed by TEM, the growth of Ni concentration in the PPX-Ni nanocomposite films also affects the oxidation state of the inorganic nanoparticles.

4 Conclusions

The growth of Ni concentration in the PPX-Ni nanocomposite films affects the oxidation state of the inorganic nanoparticles. Most of the particles in the composite films with low filler content (C = 5 vol.% of Ni) are oxidized (NiO), whereas the particles in the PPX-Ni composite with 30 vol.% of Ni are mainly metallic.

The magnetic and electrical properties of the PPX-Ni nanocomposite films are determined by their structure being of the percolation type. The well pronounced magnetic hysteresis as well as ferromagnetic ordering were observed at Ni content above the percolation threshold. On the base of obtained data the diagrams of magnetic properties of the PPX-Ni nanocomposite as a function of composition and temperature including both paramagnetic and ferromagnetic contributions were elaborated. These graphs demonstrate that variation in composition of the nanocomposite films results in significant changes of their magnetic properties. In particular, pronounced ferromagnetic phase appears at room temperature in samples with C > 15 vol.%, although introduction of Ni into PPX matrix leads to an increase of paramagnetic contribution for all studied C values (6-30 vol.%).

This work was partially supported by the Russian Foundation for Basic Research (grant #15-29-01267). The study was carried out using the equipment of the Resource Centers of Kurchatov's Complex of NBICS-Technologies.

References

[1] S. Majumdar, H. S. Majumdar, H. Aarnio, and R. Osterbacka, Phys. Status Solidi - Rapid Res. Lett. **3**, 242 (2009).
[2] E. I. Grigoriev, S. A. Zavyalov, and S. N. Chvalun, Polym. Sci. Ser. A **45**, 1308 (2003).
[3] P. K. Choudhury, S. Ramaprabhu, K. P. Ramesh, and R. Menon, J. Phys. Condens. Matter **23**, 265303 (2011).
[4] Y. Liu, S. M. Watson, T. Lee, J. M. Gorham, H. E. Katz, J. A. Borchers, H. D. Fairbrother, and D. H. Reich, Phys. Rev. B **79**, 75312 (2009).
[5] M. Grunewald, J. Kleinlein, F. Syrowatka, F. Wurthner, L. W. Molenkamp, and G. Schmidt, Org. Electron. **14**, 2082 (2013).
[6] K. Akamatsu, S. Adachi, T. Tsuruoka, S. Ikeda, S. Tomita, and H. Nawafune, Chem. Mater. **20**, 3042 (2008).
[7] E. Hirota, H. Sakakima, and K. Inomata, *Giant Magneto Resistance Devices* (Springer Science and Business Media, 2002).
[8] A. Riminucci, I. Bergenti, L. E. Hueso, M. Murgia, C. Taliani, Y. Zhan, F. Casoli, M. P. de Jong, and V. Dediu, arXiv:cond-mat/0701603 1 (2007).
[9] H. Hopf, G. N. Gerasimov, S. N. Chavalun, V. I. Rozenberg, E. L. Popova, E. V. Nikolaeva, E. I. Grogoriev, S. A. Zavjalov, and L. I. Trakhtenberg, Chem. Vap. Depos. **3**, 197 (1997).
[10] G. N. Gerasimov, V. A. Sochilin, S. N. Chvalun, L. V. Volkova, and I. Y. Kardash, Macromol. Chem. Phys. **197**, 1387 (1996).
[11] W. F. Gorham, J. Polym. Sci. Part A-1 Polym. Chem. **4**, 3027 (1966).